PUBLICATIONS OF THE ASTRONOMICAL SOCIETY OF THE PACIFIC, **117**:395–400, 2005 April
© 2005. The Astronomical Society of the Pacific. All rights reserved. Printed in U.S.A.

Optical Turbulence Profiles at Mauna Kea Measured by MASS and SCIDAR

A. TOKOVININ

Cerro Tololo Inter-American Observatory, Casilla 603, La Serena, Chile; atokovinin@ctio.noao.edu

J. VERNIN AND A. ZIAD

Laboratoire Universitaire d'Astrophysique de Nice, Parc Valrose, 06108 Nice Cedex 2, France; jean.vernin@unice.fr, aziz.ZIAD@unice.fr

AND

M. CHUN

Institute for Astronomy, University of Hawaii, 640 North Ahoku Place, Hilo, HI 96720; mchun@ifa.hawaii.edu

Received 2004 December 20; accepted 2005 January 19; published 2005 March 24

ABSTRACT. The vertical distribution of turbulence over Mauna Kea has been measured on four nights in 2002 October, simultaneously using two different instruments based on stellar scintillation—the generalized SCIDAR (scintillation detection and ranging) and MASS (multiaperture scintillation sensor). The turbulence integrals match within 20%, and the low-resolution profiles delivered by MASS correctly reveal the localization of the strongest high-altitude turbulent layers. As deduced from DIMM (differential image motion monitor), MASS, and SCIDAR measurements, optical turbulence in the first 0.7 km above the summit contributed typically half of the total integral, the latter corresponding to a seeing of 0.″5. The ground layer and free atmosphere are not correlated.

1. INTRODUCTION

Optical distortions in the terrestrial atmosphere, frequently referred to as "turbulence," are a major factor in defining the capabilities of ground-based telescopes and interferometers. Adaptive optics (AO) can compensate for the image blur caused by turbulence (seeing), but the sensitivity of this method to the intensity, vertical distribution, and speed of turbulence is such that knowledge of these characteristics becomes even more important for AO than for classical, seeing-limited observations (Roddier 1999). Thus, there is a need to monitor the vertical optical turbulence profiles (OTPs) at existing and future astronomical sites.

A classical optical method of OTP measurement is with SCIDAR (scintillation detection and ranging; Avila et al. 1997), which is based on the spatial correlation of intensity fluctuations (scintillation) produced by a double star in the pupil plane of a telescope. However, the required aperture size of the feeding optics (>1 m) and heavy data processing have precluded the use of SCIDAR for regular OTP monitoring, restricting its use to dedicated campaigns.

An alternative method of OTP monitoring relies on the analysis of the scintillation of single stars. The multiaperture scintillation sensor (MASS) has recently been developed based on this principle (Kornilov et al. 2003). The advantage of MASS is its small aperture (8–15 cm) and its simplicity; its drawback is a low vertical resolution. In this respect MASS is similar to the differential image motion monitor (DIMM), which has been adopted as standard method for measuring seeing (e.g., Vernin & Muñoz-Tuñón 1995).

It is essential to check new instruments like MASS against established techniques. This paper reports on a MASS-SCIDAR comparison conducted as part of the 2002 Mauna Kea (MK) site characterization campaign. The OTP properties at this site are also discussed.

The definitions of the turbulence parameters used in this paper are given by Roddier (1981) and in numerous other sources. The intensity of turbulence at some altitude h is characterized by the refractive index structure constant $C_n^2(h)$, measured in $\mathrm{m}^{-2/3}$. In the framework of the standard Kolmogorov-Tatarski turbulence model (Tatarskii 1971), the integral strength of turbulence $J = \int C_n^2(h)\, dh$ (in $\mathrm{m}^{1/3}$) is directly related to the half-width of the seeing-limited image ϵ in a large telescope. Throughout this paper, an ϵ at a 500 nm wavelength at zenith is used, in which case $\epsilon/1'' = (J/6.8 \times 10^{-13})^{3/5}$. The turbulence integral J in the free atmosphere (starting at 700 m above the ground) is converted to "free-atmosphere seeing" by the same formula.

In § 2 we describe the SCIDAR, MASS, and DIMM instruments and the data they obtained during the MK 2002 campaign. MASS and SCIDAR data are compared in § 3. Finally, in § 4 we give some results from OTP measurements using all three instruments.

2. INSTRUMENTS AND DATA

2.1. Generalized SCIDAR

The SCIDAR instrument was developed at Nice University and operated by J. Vernin and A. Ziad. It was installed at the

88 inch (2.2 m) telescope of the University of Hawaii (UH). It uses suitable bright binary stars as light sources and works in generalized mode, measuring all turbulence with a 20 s integration time. The vertical sampling of the profile is on a 300 m grid extending from some altitude below the mountain (to measure the ground layer correctly) to ~20 km above the site.

The principle of the generalized SCIDAR is based on the extraction of the spatial correlation of the scintillation images of binary stars. The CCD detector that records these scintillation patterns is placed in the analysis plane conjugated to some negative altitude $h_{\rm gs}$ (i.e., below the pupil). This additional propagation distance $h_{\rm gs}$ produces detectable scintillation from ground-layer turbulence, making SCIDAR sensitive to turbulence at all altitudes.

Two spatial autocorrelation functions of scintillation images, $C_{||}$ and $C_{\perp}$, are computed in the directions parallel and perpendicular to the star separation. The difference between these functions is given by Avila et al. (1997) as

$$B_{**}(x) = C_{\parallel}^{**} - C_{\perp}^{**} = \int_{-h_{\rm gs}}^{+\infty} dh\, K(x, h) C_n^2(h + h_{\rm gs}) + N(x), \qquad (1)$$

where the kernel of the integral equation $K(x, h)$ corresponds to the theoretical autocorrelation function produced by a single layer at an altitude h with a unit C_n^2, and where $N(x)$ corresponds to the experimental noise. Here $B_{**}(x)$ is measured with the SCIDAR, and the kernel $K(x, h)$ is calculated theoretically. Introducing these quantities in equation (2) then allows us to retrieve $C_n^2(h)$ by inversion using a maximum entropy algorithm. The profile thus obtained is shifted toward a higher altitude by $|h_{\rm gs}|$ and corrected to retrieve the true OTP.

The vertical resolution of the $C_n^2(h)$ profiles provided by SCIDAR has been defined by Avila et al. (1997), and more recently in the sense of FWHM by Prieur et al. (2001),

$$\triangle H = \frac{0.78}{\theta} (\lambda |h - h_{\rm gs}|)^{1/2}, \qquad (2)$$

where λ indicates the wavelength and θ corresponds to the double-star separation. This natural vertical resolution is improved by a factor of about 2 when one uses the maximum entropy technique (Vernin 1992). Indeed, when two peaks corresponding to two close altitudes are mixed together in the sense of FWHM, they can still be separated if the signal-to-noise ratio is high enough.

The CCD camera is placed at a suitable distance behind the collimating lens to give $h_{\rm gs} = -3$ km. The vertical resolution ΔH depends on the double-star separation as indicated in equation (2). Table 1 gives the list of the double stars observed during the MK campaign, in addition to the corresponding vertical resolution at the ground and at 20 km.

TABLE 1
DOUBLE STARS OBSERVED BY SCIDAR DURING THE MK CAMPAIGN IN 2002 OCTOBER

Target	Observation Period (UT)	θ (arcsec)	$\Delta H_{\rm min}$ (m)	$\Delta H_{\rm max}$ (m)
γ Del	4:30–8:30	11.9	336	940
γ Ari	9:00–13:30	7.82	512	1417
α Gem	14:00–6:00	2.68	1493	4134

NOTE.—For each star, the resolutions at the ground level ($\Delta H_{\rm min}$) and at $h = 20$ km ($\Delta H_{\rm max}$) are given according to eq. (2) for $h_{\rm gs} = -3$ km.

The images recorded with the CCD are processed in real time for the extraction of the autocorrelations $C_{||}$ and $C_{\perp}$ and then their difference, $B_{**}(x)$. Once the data are returned from the observing campaign, data analysis is then performed to extract the $C_n^2(h)$ profiles. Dome seeing has not been subtracted.

2.2. MASS

The MASS instrument was built at Moscow University under a contract with AURA (Kornilov et al. 2003). The light of a single bright star collected by a small telescope goes through a field stop and a Fabry lens. A system of four small concentric, tilted mirrors in the exit pupil splits the light between four apertures. The flux in each aperture is measured by photomultipliers with fast (17 ns resolution) photon counters. More information on MASS instruments can be found on the Web.[1]

The 1 ms photon counts accumulated in 1 minute are converted to four normal scintillation indices (one per aperture) and to six differential indices for each pair of apertures. This set of 10 numbers is fitted by a model of six thin turbulent layers at predefined altitudes of 0.5, 1, 2, 4, 8, and 16 km above the site (Tokovinin et al. 2003). Another model of three layers at "floating" altitudes is also fitted. Turbulence integrals J_i in these six (or three) layers represent the OTP measured by MASS. These two methods of OTP restoration are complementary: fixed layers is the standard, quantitative method used in this paper, whereas floating layers produce a more qualitative result, helping to localize strong layers. Turbulence near the ground does not produce any scintillation; MASS is "blind" to it and can only measure the seeing in the free atmosphere.

It has been demonstrated through simulations and experience that integral turbulence parameters such as seeing and isoplanatic angle are measured by MASS reliably (Tokovinin et al. 2003). The restoration of the OTP is straightforward in conditions involving one dominant layer, but it is more complex for cases in which multiple layers of comparable intensity are present. This procedure tends to fit data with a minimum number of layers and hence underestimates weak layers by ascribing to them zero turbulence. The restoration errors of each layer are ~10% of the total integral. Under conditions of moderate and strong scintillation (not encountered in this campaign), the

[1] See http://www.ctio.noao.edu/~atokovin/profiler.

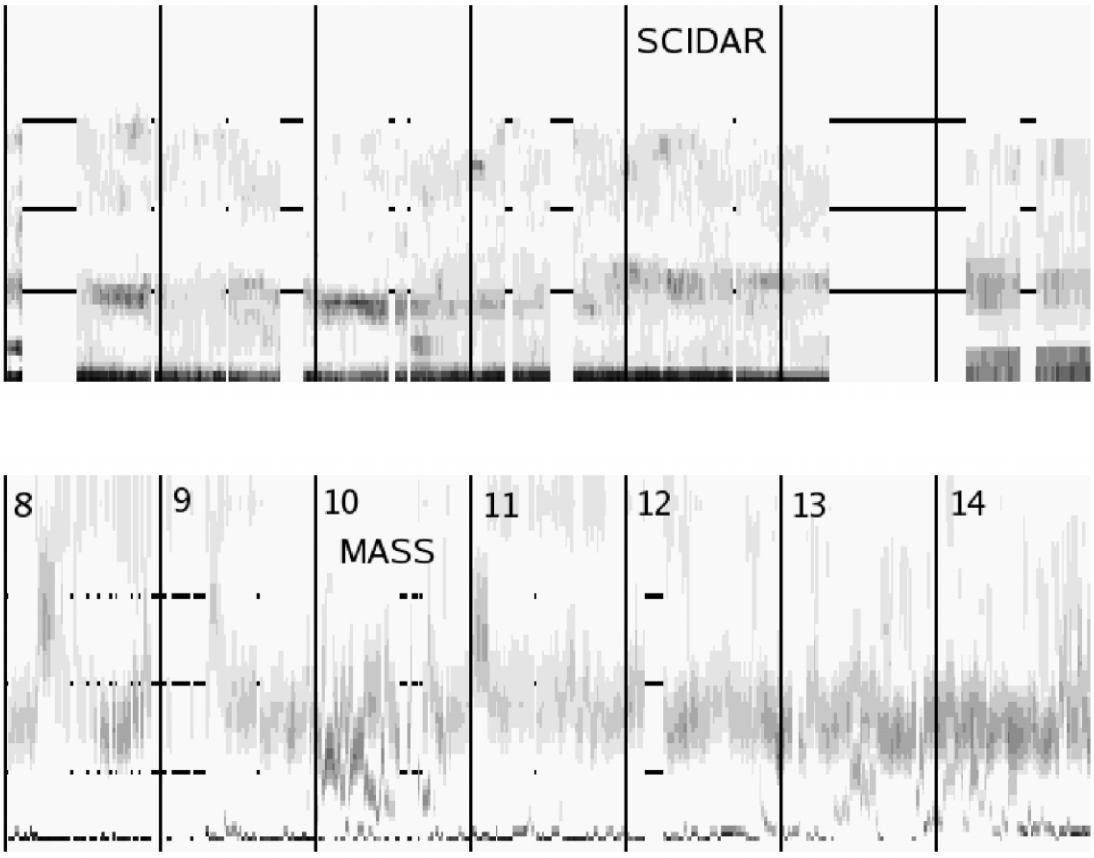

FIG. 1.—Qualitative comparison of turbulence profiles on October 22/23 as measured by (*a*) SCIDAR and (*b*) MASS. A square-root stretch with arbitrary normalization is used in both plots. Black horizontal lines mark the altitudes 5, 10, and 15 km above the site; vertical lines denote UT hours. The period from 8:00 to 15:00 UT is plotted.

MASS restoration procedure based on the weak-scintillation theory requires some modification, otherwise the free-atmosphere seeing is overestimated.

In OTP restoration, turbulence located between the predefined fixed layers is redistributed to adjacent layers in suitable proportions. Simulations have shown that the MASS response functions are close to triangular (Tokovinin et al. 2003). Thus, turbulence intensity in a 2 km "MASS layer" is in fact an integral of the OTP multiplied by the response function that starts from zero at 1 km, reaches 1 at 2 km and drops again to zero at 4 km.

The MASS instrument was installed at the 24 inch (0.6 m) UH telescope. An additional system of two lenses was placed between MASS and the telescope to obtain the desired diameters of the circular apertures projected on the telescope mirror (20, 37, 68, and 130 mm). The telescope was pointed to a bright single star near zenith, and a 1–2 hr sequence of 1 minute measurements was started. Owing to good telescope tracking and MASS's wide 3′ field, the instrument could be left unattended during these sequences.

In principle, MASS could measure the near-ground turbulence (hence, total seeing) if its apertures were conjugated to a defocused image of the telescope pupil, as with generalized SCIDAR (Kornilov et al. 2003). Telescope tracking errors and diffraction on the edge of the pupil limit the usefulness of this mode. We took advantage of the large aperture and good tracking of the 24 inch telescope and experimented with MASS's generalized mode. A comparison with a DIMM instrument located outside the dome has shown that "generalized" MASS measurements often overestimated the seeing. Possible reasons for this discrepancy include instrumental effects, very crude modeling of low turbulence by a layer at zero altitude, and turbulence inside the telescope dome.

2.3. DIMM

The two portable DIMM instruments used in the MK 2002 campaign are similar to the Robo-DIMM seeing monitor developed at the Cerro Tololo Inter-American Observatory (Walker et al. 2003). In this DIMM, a 25 cm Meade telescope is covered by a mask with two 6 cm holes. One of the holes has a thin-wedge prism to separate the stellar images in the focal plane, where a frame-transfer CCD takes a series of short exposures. The minimum exposure time is 5 ms. Interlaced 5 and

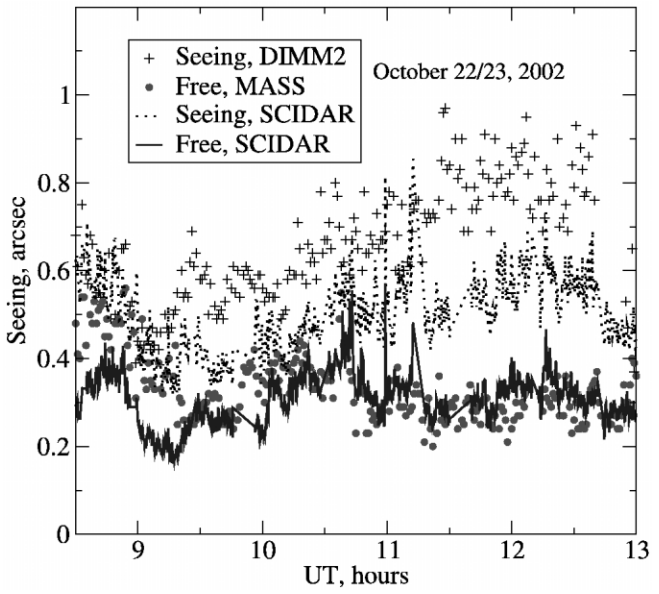

FIG. 2.—Evolution of the total and free-atmosphere seeing on October 22/23, according to three independent instruments. [*See the electronic edition of the PASP for a color version of this figure.*]

10 ms exposures were taken over 1 minute to correct the seeing for the finite-exposure bias, using the method given in (Tokovinin 2002).

The DIMM-1 instrument was installed on a tripod near the 24 inch dome, at an altitude of ~1.5 m above the ground. DIMM-2 was installed on the coudé roof of the 88 inch telescope, in proximity to its dome and about 13 m above the ground. We observed that DIMM-1, presumably affected by turbulence near the ground, sometimes indicated significantly worse seeing than DIMM-2. Only DIMM-2 data are used in this paper.

2.4. Data Overview

MASS and SCIDAR worked jointly at MK on 2002 October 20–23 (local dates of the beginning of each night). Some MASS data were also obtained on October 19 and during additional runs on November 22, 23, and 26. In this paper, only the data obtained on October 20–23 are used. There were thin cirrus clouds on October 22 (before 8:00 UT) and 23 (whole night), yet the MASS results are considered valid, because slow flux variations caused by cirrus are filtered out in signal processing.

The temporal coverage was not continuous: gaps in SCIDAR data are related to the change of double stars, and gaps in the MASS data occurred between the acquisition series. Only data collected simultaneously are selected for comparison. More specifically, a period of October 22, between 8:30 and 13:00 UT, is chosen because of good coverage by both SCIDAR and MASS and because of significant OTP variations during that period. SCIDAR and MASS looked at different stars, thus sampling different parts of the atmosphere at any given instant. Each instrument was calibrated independently. No normalization or other "adjustment" was applied to the data sets discussed below.

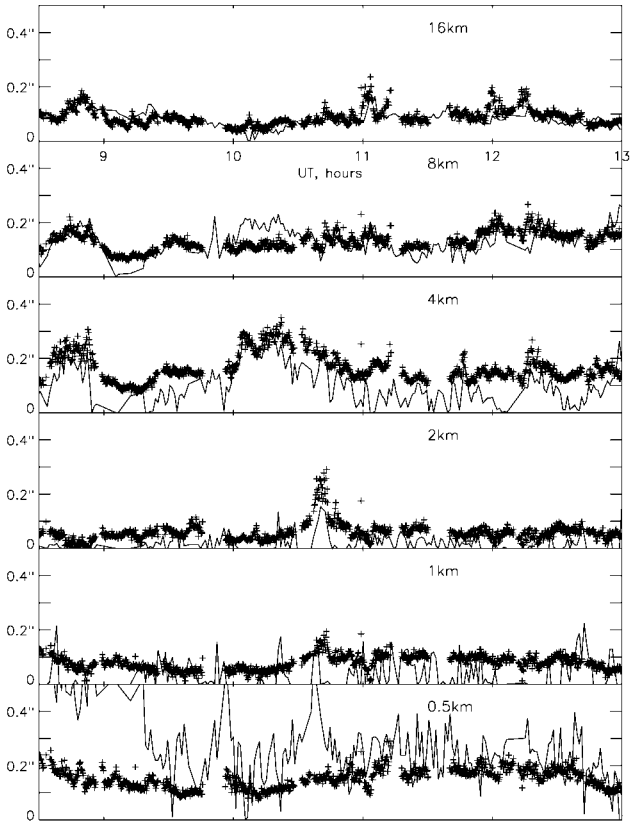

FIG. 3.—Seeing produced by each of the six "slabs" (vertical axis in arcsec) as a function of UT time according to MASS (*solid lines*) and SCIDAR (*crosses*) on 2002 October 22 from 8:30 to 13:00 UT.

3. MASS-SCIDAR COMPARISON

A first qualitative comparison is given in Figure 1 as halftone profiles with square-root stretch to accentuate weak turbulence. The altitude scale is linear, starting at the mountaintop (4200 m above sea level). The MASS "floating layer" data were used to produce this figure in order to compare the localization of strong layers with SCIDAR.

We also compared the turbulence integrals measured by three instruments. In Figure 2 the free-atmosphere seeing given by SCIDAR is computed by integrating the profiles from 700 m upward; it agrees very well with the MASS data. The total seeing measured by DIMM agreed well with the seeing measured by SCIDAR until 9:30 UT, when DIMM started to show worse seeing. We believe that DIMM could be affected by additional turbulence created by the wake of the 88 inch dome.

A more quantitative comparison is made by integrating the products of SCIDAR OTPs and MASS triangular response functions to match the vertical resolution of MASS. The integrals J are transformed into the seeing produced by each layer. The results for one night are plotted in Figure 3 as a function of time. No time rebinning or averaging was applied. Note the very good agreement for 8 and 16 km layers and the overestimation of the 0.5 km layer by MASS, and also its frequent

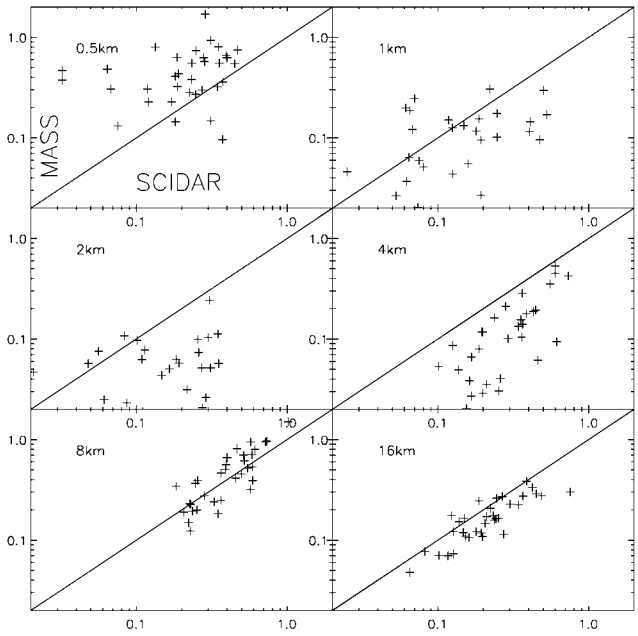

FIG. 4.—Comparison of hourly-averaged turbulence intensities (in 10^{-13} $m^{1/3}$ units) for the whole data set, with SCIDAR on the horizontal axis and MASS on the vertical axis.

measurements of unrealistic zero seeing in some layers. These features are explained by the restoration technique, in which the total integral is well constrained by the differential indices, but its distribution among six predefined layers is not always correct. The main error is an excessive signal in low layers, at the expense of higher layers. Generally, OTP restoration errors increase with decreasing layer height.

Given the high noise in the data (especially those of MASS), the natural "noise" of turbulence (intermittency), and different viewing directions, it makes sense to compare averaged quantities. To this end, we averaged the intensities of turbulent layers J over 1 hr time intervals for both instruments. Only data points for which both instruments are synchronous within 1 minute are taken into consideration, and a minimum number of averaged profiles during any hour is set to 20. Hence, not all hours produce useful comparisons. Scatter plots for all layers and all 1 hr average points are given in Figure 4.

In Table 2 we compare the average turbulent integrals measured on each night and in each layer. The last column compares the averages for the whole period. The agreement between the integrals is impressive, despite completely independent calibrations of MASS and SCIDAR. We again note that MASS systematically underestimated weak layers at 2 and 4 km and overestimated the lowest layer (0.5 km).

4. TURBULENCE PROFILE AT MAUNA KEA

The properties of the OTP over Mauna Kea as derived from the MK 2002 campaign are discussed here. Despite limited statistics, it is the best available data set for this major international observatory, where several projects on AO and interferometry are being implemented.

In Table 3 we give the levels of the cumulative distributions of seeing computed from the turbulence integrals in the ground layer (GL), in the free atmosphere (FA), and for the total atmosphere (TOT). The seeing derived from 6530 SCIDAR profiles is marked with asterisks. We also derive the FA integrals from 2250 MASS profiles and estimate the total and GL integrals from 924 points in common between MASS and DIMM. The good agreement of FA integrals between MASS and SCIDAR has already been established. DIMM measured somewhat worse total seeing than SCIDAR, as evident in Figure 2 and Table 3.

TABLE 2
COMPARISON OF NIGHTLY AVERAGE TURBULENCE INTEGRALS

Measurement (km)	2002 Oct 20/21	2002 Oct 21/22	2002 Oct 22/23	2002 Oct 23/24	All
Number[a]	5	10	10	9	34
16 S	0.16*	0.32*	0.15*	0.30*	0.24*
16 M	0.13	0.24	0.12	0.20	0.18
8 S	0.66*	0.43*	0.27*	0.47*	0.43*
8 M	0.94	0.56	0.26	0.43	0.49
4 S	0.38*	0.37*	0.29*	0.17*	0.30*
4 M	0.14	0.19	0.14	0.07	0.13
2 S	0.09*	0.15*	0.10*	0.25*	0.15*
2 M	0.06	0.08	0.02	0.05	0.05
1 S	0.06*	0.13*	0.12*	0.32*	0.17*
1 M	0.14	0.10	0.04	0.15	0.10
0.5 S	0.22*	0.15*	0.24*	0.35*	0.24*
0.5 M	0.18	0.37	0.70	0.53	0.48
Total S	1.58*	1.56*	1.17*	1.86*	1.53*
Total M	1.61	1.54	1.29	1.43	1.45

NOTE.—Turbulence integrals (in 10^{-13} $m^{1/3}$) measured by SCIDAR (S) and MASS (M) in each layer. Asterisks identify the seeing derived from 6530 SCIDAR profiles.

[a] Number of 1 hr averages.

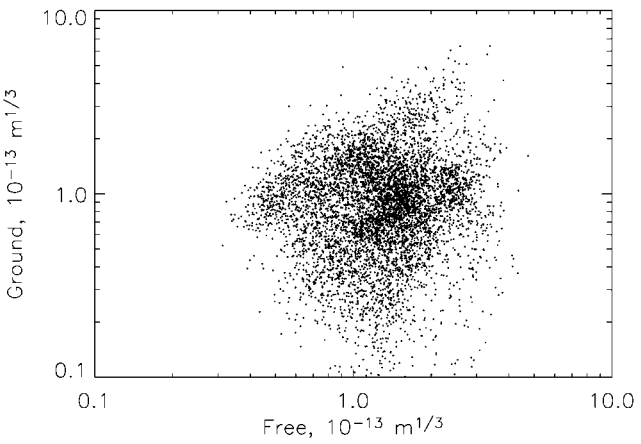

FIG. 5.—The lack of correlation between turbulence integrals in the ground layer (below 700 m) and in the free atmosphere is demonstrated with SCIDAR data.

We warn the reader that this statistic is derived from only four nights and cannot be used to characterize the MK site. However, some OTP features revealed by the MK 2002 campaign deserve comment. It is clear that the seeing was not dominated by turbulence at any specific altitude, with all layers showing contributions of comparable magnitude (Table 2). The contributions of FA and GL are also comparable. The GL is responsible for some 40% of the total integral, according to SCIDAR (54% according to MASS-DIMM). The median total integrals correspond to a seeing of 0.″51 (SCIDAR) or 0.″63 (DIMM).

Since the physics governing the generation of turbulence in the GL and FA is different, the corresponding integrals are expected to be statistically independent. This does seem to be the case (Fig. 5). Thus, the OTP can be modeled as independent combination of the GL and FA components.

The OTP parameters at MK are similar to those at other good, well-studied astronomical sites. For example, 43 microthermal balloon soundings at Cerro Pachón in Chile distributed throughout one year revealed median integrals in GL and FA of 1.14×10^{-13} and 1.73×10^{-13}, respectively (Avila et al. 2000). The last number has been confirmed by 21 nights of monitoring with MASS in 2003 January.

TABLE 3
CUMULATIVE DISTRIBUTION OF SEEING

Probability	10%	25%	50%	75%
GL (S)	0.14*	0.22*	0.29*	0.36*
GL (D, M)	0.11	0.29	0.44	0.57
FA (S)	0.25*	0.30*	0.37*	0.43*
FA (M)	0.26	0.32	0.38	0.45
TOT (S)	0.37*	0.43*	0.51*	0.59*
TOT (D)	0.48	0.54	0.63	0.73

NOTE.—Cumulative distribution of seeing (in arcseconds) created by turbulence in the ground layer below 700 m (GL) in the free atmosphere (FA) and total (TOT) according to SCIDAR (S), MASS (M), and DIMM (D). Asterisks identify the seeing derived from 6530 SCIDAR profiles.

5. CONCLUSIONS

Two independently calibrated instruments, MASS and SCIDAR, show very good agreement (better than 20%) of the turbulence integral in the free atmosphere. The turbulence intensities in the highest layers (8 and 16 km) also agree very well, whereas lower layers are restored by MASS with larger errors. Overall, MASS is shown to be a viable tool for the measurement of the turbulence integral (hence, seeing) in the free atmosphere and for localizing strong turbulent layers. This simple technique finds increasing applications in site testing (Skidmore et al. 2004; Lawrence et al. 2004) and OTP monitoring at existing observatories.

We found that under favorable conditions of 0.″5 seeing encountered in 2002 October, all atmospheric layers at MK made comparable contributions to the turbulence integral. About half of the integral was caused by turbulence below 0.7 km, which was not correlated with the free atmosphere.

We acknowledge the funding sources that provided support for the MK 2002 campaign: Gemini Observatory, US Air Force Research Lab, the University of New Hampshire, and the University of California, Santa Cruz. DIMM instruments were operated by Jake Jacobson. We are grateful to the referee, J.-L. Prieur, for his constructive comments.

REFERENCES

Avila, R., Vernin, J., & Masciadri, E. 1997, Appl. Opt., 36, 7898
Avila, R., et al. 2000, Proc. SPIE, 4007, 721
Kornilov, V., et al. 2003, Proc. SPIE, 4839, 837
Lawrence, J. S., et al. 2004, Nature, 431, 278
Prieur, J. L., Daigne, G., & Avila, R. 2001, A&A, 371, 366
Roddier, F. 1981, Prog. Opt., 19, 281
Roddier, F., ed. 1999, Adaptive Optics in Astronomy (Cambridge: Cambridge Univ. Press)
Skidmore, W., et al. 2004, Proc. SPIE, 2004, 5489, 154
Tatarskii, V. I. 1971, The Effects of the Turbulent Atmosphere on Wave Propagation (US DOC TT-68-50464; Jerusalem: Israel Program for Scientific Translations)
Tokovinin, A. 2002, PASP, 114, 1156
Tokovinin A., Kornilov, V., Shatsky, N., & Voziakova, O. 2003, MNRAS, 343, 891
Vernin, J. 1992, in Wave Propagation in Random Media (Scintillation): Invited Papers, ed. V. I. Tatarskii, A. Ishimaru, & V. U. Zavorotny (Bellingham: SPIE Press), 248
Vernin, J., & Muñoz-Tuñón, C. 1995, PASP, 107, 265
Walker, A., et al. 2003, Proc. SPIE, 4840, 509